Article

Journal of
Nanoscience and Nanotechnology
Vol. 17, 4936–4945, 2017
www.aspbs.com/jnn

The Morphology of TiO_2 Nanotube Arrays Grown from Atomically Peened and Non-Atomically Peened Ti Films

Samira Farsinezhad[1], Arash Mohammadpour[1], Mourad Benlamri[1], Ashley N. Dalrymple[1], and Karthik Shankar[1, 2, *]

[1] *Department of Electrical and Computer Engineering, University of Alberta, Edmonton, AB, T6G 2V4, Canada*
[2] *National Institute for Nanotechnology, National Research Council, 11421 Saskatchewan Drive, Edmonton, AB, T6G 2M9, Canada*

The growth of TiO_2 nanotube arrays (TNTAs) on non-native substrates is essential for exploiting the full potential of this nanoarchitecture in applications such as gas sensing, biosensing, anti-fouling coatings, low-cost solar cells, drug-eluting bimedical implants and stem-cell differentiators. The direct formation of anodic TNTAs on non-native substrates requires the vacuum deposition of a thin film of titanium on the substrate followed by subsequent electrochemical anodization of the film. In this report, we studied the effect of atomic peening on the formation of Ti thin films on technologically important non-native substrates. We compared the structure and morphology of evaporated and sputtered Ti films, and correlated them to the morphology of the vertically oriented TiO_2 nanostructures that resulted subsequent to anodization of those films. We calculated a minimum value of 1.33 eV/atom for the energy of reflected neutral Ar species arriving at the substrate when a chamber pressure of 1 mTorr is used during the sputter deposition of Ti. Previous approaches relied on substrate heating to elevated temperatures during Ti thin film deposition or ion-beam assisted Ti thin film deposition as a prerequisite to form TiO_2 nanotube arrays (TNTAs). We demonstrated TNTAs on a variety of substrates at room temperature using both evaporated and sputtered Ti films without recourse to ion-beam sources. Evaporated Ti films were found to possess small grain size and high local surface roughness, which resulted in nanotubes with extremely rough sidewalls. Ti thin films formed by Ar^+ ion sputtering at commonly used chamber pressures of 7–20 mTorr at substrate temperatures ranging from room-temperature to 250 °C possessed a highly rough surface and three-dimensional grains, which precluded the formation of ordered nanotubes upon anodization due to highly non-uniform pore nucleation processes. In contrast, Ti thin films sputtered at low chamber pressures of 0.8–2 mTorr had a low surface roughness due to the atomic peening process. Such films, even when deposited at room temperature, resulted in ordered nanotube arrays upon anodization.

Keywords: DC Sputtering, Vacuum Deposition, Si Wafers, Polymeric Substrates, Electron Beam Evaporation, Ion Beam Sputtering, Zone Models.

1. INTRODUCTION

TiO_2 nanotubes grown on titanium foils[1, 2] have been demonstrated to be employable in a wide range of applications such as catalysts, photocatalysts, photovoltaics, interferometric sensors, immunoassays, electrochemical sensors, supercapacitors, etc. due to the unique combination of properties such as *n*-type semiconducting behavior, a wide electronic band gap, high surface area, high refractive index, large capacitance and moderate electron mobility.[3–14] However, highly ordered and vertically oriented titanium dioxide nanotube arrays grown on non-native substrates are more advantageous in specialized applications where Ti foils are unsuitable.[1, 2, 15–19] Due to their transparency, glass substrates and transparent conductive oxide (TCO)-coated glass substrates are extensively used in the photovoltaic, display and optical sensing industries. Stainless steel is the material of choice in industrial tubing due to its mechanical and chemical properties. Plastic substrates are necessary for flexible applications; among plastics, polyimide substrates (e.g., Kapton®) are

*Author to whom correspondence should be addressed.

 1533-4880/2017/17/4936/010 doi:10.1166/jnn.2017.13310

popular for their relatively high temperature resistance. Silicon substrates are typically used for on-chip integrated electronic and photonic circuits, and in MicroElectroMechanical Systems (MEMS).

In addition to being highly functional and self-ordered, TNTAs grown by a bottom-up process are relatively cheap to produce in comparison to standard micro- and nanoarchitectures requiring top-down lithographic techniques. The length and pore size of TNAs on native Ti foil substrates and the effect of various electrolytes such as organic and aqueous recipes on the morphology, ordering and surface area of TNAs have been extensively investigated.[2, 11] The Ti foils used in such studies are hot-rolled uniform substrates with flat grains 10–100 μm in size. In contrast, the grain sizes in thin films of Ti on non-native substrates are orders of magnitude lower. Several groups have demonstrated the formation of titania nanotubes of widely varying structure and morphology on Ti thin films deposited on conductive glass[20] and silicon and flexible polymeric substrates using different film deposition and heating conditions.[21, 22] However, there very few reports that connect the Ti film growth process and the properties of the Ti film to the structure and morphology of the resulting TNTAs. Here, we use quantitative metrics for the film deposition process to identify optimal film growth conditions. We also conduct a fundamental study of the effect of the deposition parameters of the Ti thin films on the morphology of the resulting TiO_2 nanotube arrays. Prior reports indicated that smooth surfaces with large grains are more favorable for nanotube formation. However, our results show that smoothness is significantly more important that grain-size in order to obtain nanotubes as opposed to a nanoporous structure. A large grain-size, especially when randomly oriented, is associated with a larger dispersity in the shape and size of the nanotubes, and can even lead to the formation of random nanopores. Almost monodisperse nanotube arrays are formed on silicon substrates,[23] which not coincidentally, also result in Ti thin films with the minimum surface roughness. Furthermore, nanotube arrays can be achieved using simple, high-throughput DC sputtering at room temperature by performing the deposition at low chamber pressures, thus benefiting from the atomic peening mechanism. The effect of thin film quality on the formation of highly ordered TiO_2 nanotube arrays on glass, fluorine-doped tin oxide (FTO) coated glass and silicon wafers is presented here. We show that by specifying the sputtering rate and pressure during deposition, the morphology of titanium film on a variety of substrates is controllable.

2. EXPERIMENTAL SECTION

Glass, FTO-coated glass (hereafter referred to as FTO:glass) and Kapton substrates cleaned by sequential ultrasonication in detergent, water and alcohol. Silicon wafers were cleaned by immersion in a piranha solution for 15 min followed by rinsing and drying.[24] Both DC magnetron sputtering and electron beam evaporation were used to deposit Ti thin films 250 nm to 2 μm in thickness. When sputtering was used, the deposition was performed at room temperature, 250 °C and 700 °C and at pressures ranging from 0.8 mTorr to 20 mTorr from a 99.99% pure Ti target (diameter = 7.68 cm) at a power of 150 W using 50 sccm of argon flow. For substrates heated to 700 °C, quartz was used as the substrate instead of glass and FTO:glass because of its higher temperature resistance. When substrate heating was used during the vacuum deposition of Ti films, the substrates were cooled to room temperature in vacuum at an approximate rate of 1 °C min^{-1}. The deposition rate for different samples varied from 0.045 nm s^{-1} to 0.23 nm s^{-1}. The anodization of Ti films was performed potentiostatically at 40 V in a two-electrode geometry using an ethylene glycol-based electrolyte containing 0.3 wt% NH_4F and 4–9% DI water. The Ti film served as the working electrode while a graphite rod of diameter 3 mm was used as the counter-electrode. When atoms ejected from the target reach the surface of the substrate at normal incidence, they lose their energy in the ns timeframe via Lennard-Jones interactions. On the other hand, ejected atoms incident on the substrate at oblique angles conserve parallel momentum,[25] and therefore the angle of the sputter gun plays an important role in surface diffusion. In this work, the magnetron sputter gun was directed at the substrate at an angle 10.2° from the substrate normal. After deposition but prior to anodization, to prevent the faster etching at the air-electrolyte interface and the sample edges, such regions of high electric field concentration were sealed with parafilm at 75 °C to construct a square window (1.5 cm^2) and anodization was restricted to the Ti film contained in this window. The distance between the sample and the cathode was approximately 4 cm, and a DC power supply was used to drive the reaction. The choice was made to use organic electrolytes as they have the ability to produce nanotubes with significantly higher lengths and pattern ordering than aqueous solutions due to the reduced chemical dissolution of the nanotube surfaces, thinner barrier layers and more controlled pitting/nucleation processes. Once the anodization had concluded, the samples were immersed in ethanol for 30 seconds and dried using a nitrogen gun. The surface morphology of the deposited film and the anodized titanium were determined using atomic force microscopy (AFM), transmission electron microscopy (TEM) and field emission scanning electron microscopy (FESEM).

3. RESULTS AND DISCUSSION

3.1. Effect of Temperature on the Surface Morphology of Ti Films Before Anodization

Figure 1 shows the well-documented effect of substrate temperature in engineering a smooth, uniform Ti film

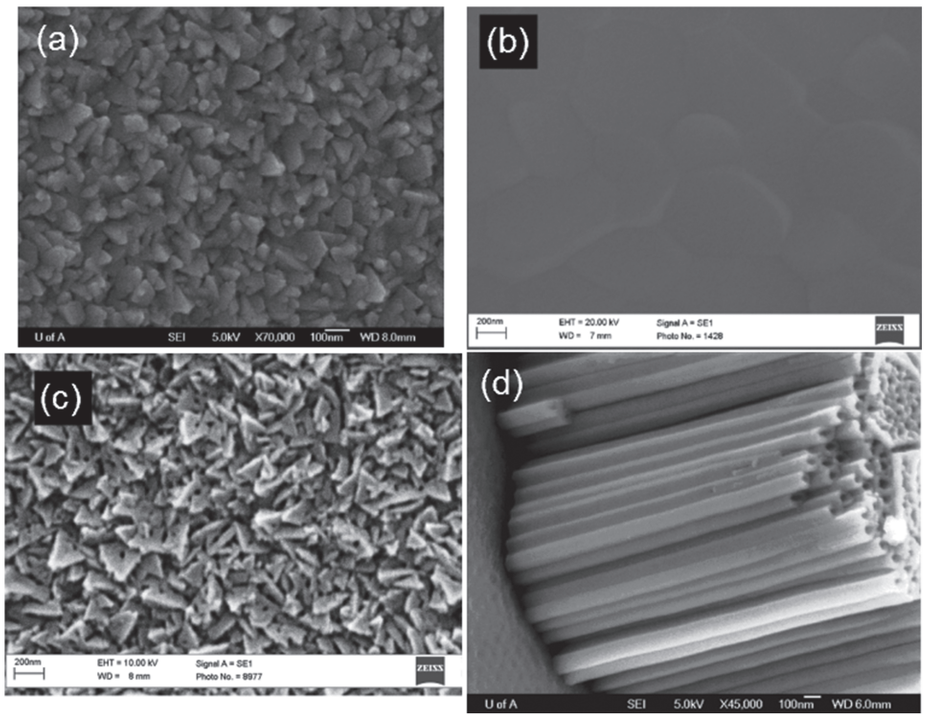

Figure 1. Effect of substrate temperature on the morphology of 500 nm-thick titanium films deposited on quartz by DC sputtering at a chamber pressure of 7 mTorr (a) top-view SEM images of a Ti thin film coated on a substrate maintained at room temperature (b) top-view SEM image of a Ti thin film coated on a substrate heated to 700 °C (c) top-view SEM image of TiO_2 nanopores resulting from the room-temperature deposited film shown in (a) after electrochemical anodization and (d) Profile-view SEM image of ordered TiO_2 nanotubes formed upon anodization of the Ti film shown in (b) deposited on to the substrate at 700 °C.

morphology. DC sputtering of a few hundred nanometers of Ti on quartz and other substrates at room temperature results in a rough, non-uniform film with three-dimensional grains with an average size of 50 nm protruding out of the plane of the substrate (Fig. 1(a)). When such rough films are subjected to electrochemical anodization, the extremely non-uniform field-assisted migration and etching processes result in the formation of an irregular, randomly organized porous structure (Fig. 1(c)) in lieu of self-organized, vertically aligned TiO_2 nanotube arrays. For this reason, several reports resorted to substrate heating to engineer a more uniform film morphology. For the quartz substrates and typical DC sputtering parameters used here, we found that a substrate temperature as high as 700 °C was required to produce Ti films of sufficient quality (Fig. 1(b)) that resulted in highly ordered nanotube arrays upon anodization (Fig. 1(d)). The quality of the Ti film here is defined by smoothness and by grain size. The Ti films deposited on to a quartz substrate heated to 700 °C had an area-weighted average grain size of 200 nm and the grains were flatter with minimal protrusion from the plane of the substrate. An interesting observation about the low temperature anodized Ti films in Figure 1(c) is that the majority of grains exhibit one pore per grain irrespective of size and orientation; the exception being the grains oriented almost orthogonally to the substrate along the surface normal, which exhibit either no pore formation or multiple pores.

Since ordered nanotube arrays are obtained on smooth, large-grained Ti foil substrates, large grains and film smoothness have both been deemed desirable, but we have recently shown that film smoothness plays a more significant role than grain size in ensuring the uniform pitting needed for nanotube formation.[23, 26] Surface diffusion of the Ti adatoms on the substrate, self-diffusion of the Ti atoms and the level of stress in the thin film are the main processes that must be optimized in order to achieve both smoothness over large areas and good adhesion to the substrate during thin film deposition. These three processes are defined by deposition conditions as well as the nature of the film and substrate material. For films thicker than 10 nm, the final film morphology that presents itself during electrochemical anodization is determined primarily by the self-diffusion of Ti atoms over other Ti atoms. Due to its importance in determining the requisite Ti film morphology on non-native substrates for TiO_2 nanotube formation, we shall here introduce quantitative metrics to measure self-diffusion.

At high temperatures, adatoms and adsorbate species have high mobility and the probability of diffusion will be increased[27] due to which film roughness is decreased. Studies conducted by Kalantar-Zadeh and colleagues,[28]

Grimes and colleagues[17, 29] and Schmidt-Mende and colleagues required substrate temperatures during Ti deposition of *ca.* 500 °C in order to achieve TNAs using Ti films deposited by magnetron sputtering. Kalantar-Zadeh and colleagues showed that at lower substrate temperatures, three dimensional grains were obtained during Ti film deposition whose anodization resulted in irregular nanopores instead of nanotubes. Higher substrate temperatures enabled the thermally activated growth of flatter plate-like grains whose anodization resulted in nanotube formation. The problem however with using high temperatures to generate Ti films suitable for transformation into TiO_2 nanotubes is that glass or FTO:glass cannot withstand temperature higher than 500 °C. Moreover, such temperatures exceed the softening/melting point of even the most resilient plastics such as polyimide thus rendering the temperature-assisted Ti film deposition process incompatible with flexible polymeric substrates.

The surface diffusion length is predicted by theory to be given by:[30]

$$\Lambda = \frac{1}{2}\sqrt{\frac{a^3\varpi}{r}\exp\left(\frac{-E_h}{kT_f}\right)} \quad (1)$$

where a_d is the average distance between adatoms (approximated by the lattice constant of Ti that is equal to 0.2951 nm at 298 K),[31] r is the deposition rate, ω is the lattice vibration frequency, E_h is the energy for self-diffusion, k is the Boltzmann constant and T_f is the temperature of the film. The energy barrier for hopping is typically one fifth the activation energy required to escape from the film.[32] From the enthalpy of vaporization of Ti at room temperature (7.097×10^{-19} J/atom), E_h is estimated to be 0.88 eV. The vibrational frequency (kT_f/h) is taken to be 0.63×10^{13} s^{-1}.

Equation (1) explains the observation in Figure 1 of the strong effect of substrate heating on the morphology of the Ti thin films as well as the resulting anodic TiO_2 nanotube arrays. Assuming the energy imparted to the substrate by sources other than direct heating to be negligible, the grains in the growing Ti film are larger and flatter at higher substrate temperatures due to correspondingly large surface- and self-diffusion lengths. For the deposition rate used (0.9 nm s^{-1}), Eq. (1) predicts an approximate grain size of 0.03 nm for Ti deposition at room temperature and 3.5 μm for Ti deposition at 700 °C. We see from Figures 1(a and b) that Eq. (1) tends to underestimate the grain size at lower temperatures and overestimate it at high temperatures. There are three reasons for this. Firstly, studies of Ti deposition on *W* surfaces have shown that the activation energy barrier for hopping on Ti surfaces has been found to better fit the relation $E_h = 0.1E_b$,[33, 34] where E_b is the Ti work function (~4.0 eV)—which results in a lower activation barrier. Secondly, at temperatures above 150 K, isolated grains decay through thermal motion such that only grains with a size larger than 3.3 nm are stable at room temperature.[35] Thirdly, while the self-diffusion activation barrier in the bulk of the grain is lower than predicted by Eq. (1), the activation barrier for diffusion along and across grain boundaries is much higher with values in the range 1.11–1.21 eV.[35] A consequence of the aforementioned three factors is that at elevated substrate temperatures, the increase in grain size of the precursor Ti films is less than predicted from theory and therefore substrate heating constitutes an inefficient way of improving the quality of the final resulting anodic TiO_2 nanotubes.

3.2. Effect of the Deposition Technique and Chamber Pressure During Deposition

Surface diffusion and self-diffusion during film growth are key parameters that control the morphology, crystallographic orientation and surface roughness of the final thin films. These help to explain the differences in the morphology of Ti films (Fig. 2) deposited by different vacuum deposition methods and under different conditions. In Figures 2(a through f), sputtering Ti at room temperature is seen to generate films with a columnar microstructure. However, the grain size is clearly larger, while film roughness and pinhole density are clearly smaller, in films sputtered at a chamber pressure of 1 mTorr (rms roughness measured by AFM to be in the range 3.5–6.5 nm) compared to 20 mTorr. On the other hand, evaporated Ti films were found to be intermediate in grain size between the former two sputtered films. Upon anodization, the Ti films sputtered at 20 mTorr did not result in TiO_2 nanotubes as shown in Figure 2(c) but instead produced a disordered randomly porous film. Ti films sputtered at 1 mTorr and evaporated Ti films did yield nanotubes as seen in Figures 1(f and i) respectively but with one key difference in morphology; the evaporated films resulted in nanotubes with highly ridged and much rougher walls as opposed to the much smoother nanotube walls obtained from anodization of the 1 mTorr sputtered films. Films deposited using both DC sputtering and electron beam evaporation at room temperature as well as at higher temperatures (tested up to 250 °C) were found to have good adhesion with a variety of substrates (glass, FTO:glass, Si) at 1 mTorr, but not at 20 mTorr. At low pressures the films were so well-adhered that when 2 μm-thick films were immersed in an electrolyte, they did not delaminate even when deposited at room temperature.

As we and others have shown in previous reports,[20, 23, 26, 36] the formation or non-formation of nanotubes is highly dependent on the morphology and structure of the Ti films. Electric fields during the anodization process are concentrated at the film asperities. If the height of the asperities and their spacing on the surface are small (< 10 nm), the non-uniform electric fields can produce a leveling of the asperities through the halogen acid-mediated electropolishing process. However when

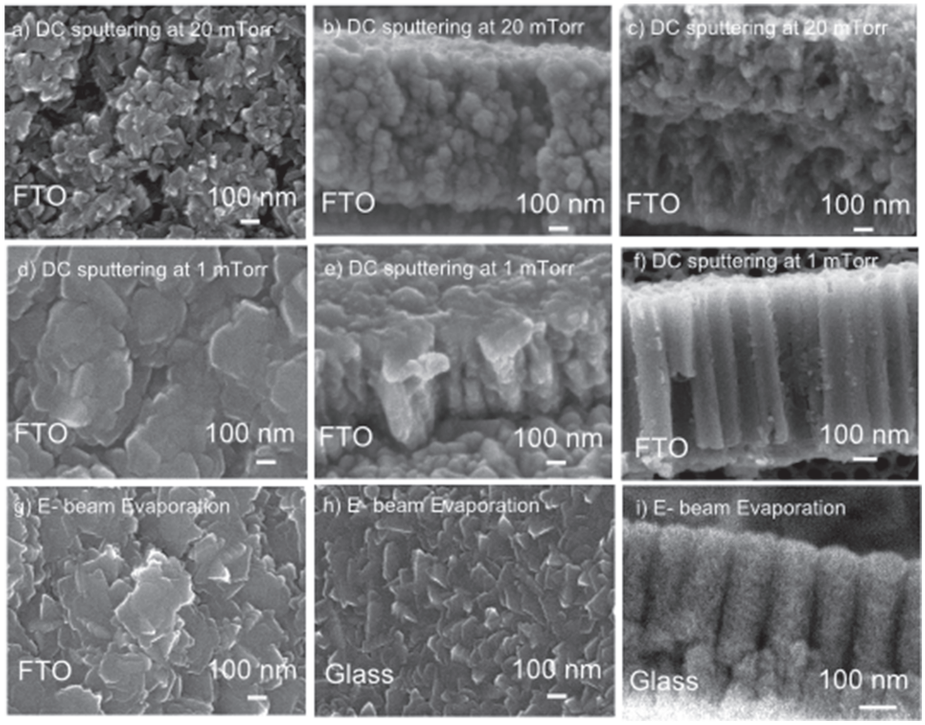

Figure 2. Morphology of 500 nm-thick titanium films (before and after anodization) deposited at room temperature on glass and FTO-coated glass substrates using DC sputtering with a deposition rate of ~0.1 nm s^{-1} and using electron beam evaporation with a deposition rate of 0.17 nm s^{-1} (a–c) top view, cross-section and cross-section upon anodization respectively of sputtered Ti films deposited at a chamber pressure of 20 mTorr (d–f) top view, cross-section and cross-section upon anodization respectively of sputtered Ti films deposited at a chamber pressure of 1 mTorr and (g–i) morphology of 500 nm of titanium deposited using electron beam evaporation (chamber pressure ~10^{-6} torr) on (g) FTO (h) glass (i) after anodization.

the asperities are larger in height and spacing, the electropolishing action is insufficient in leveling the surface due to which surface non-uniformities result in non-uniform pitting and nanotube nucleation processes. Here, we seek to understand the effect of the atomic peening process on the morphology of the Ti films deposited on different substrates and their relation to the anodic growth of ordered TiO_2 nanotube arrays. The goal here is to establish a reproducible set of non-onerous conditions (i.e., low substrate temperatures, reasonable throughput) for the formation of ordered TiO_2 nanotubes on the widest set of non-native surfaces including flexible polymeric substrates.

For evaporated Ti films, the energy of condensation of Ti from the vapor phase to the solid phase is supplied to the film without losses to the ambient (due to the low chamber pressure of ~10^{-6} torr during evaporation), which in turn is available to atoms in the film for surface diffusion and self-diffusion processes. This energy influx J_c into the film due to condensation is given by the relation[37]

$$J_c = q_c \rho R_{dep} \tag{2}$$

where q_c is the heat of condensation, which for Ti is of the order of 9.84×10^3 kJ kg^{-1} ($E_c = 4.89$ eV/atom), ρ is the mass density of the film and R_{dep} is the deposition rate. For an evaporation rate of 1 nm s^{-1}, J_c is approximately 43.59 $Jm^{-2}s^{-1}$. Since the Ti evaporation target is at a much higher temperature (T_T) than the substrate (T_S), the substrate and film also experience radiative heating given by[37]

$$J_r = \varepsilon\sigma(T_T^4 - T_S^4) \tag{3}$$

where ε is the emissivity of the target and σ is the Stefan-Boltzmann constant.

During thin film deposition by sputtering, the energy imparted to the film/substrate is a function of the chamber pressure, which is typically 3–4 orders of magnitude higher than in a thermal evaporator in order to sustain a plasma. In addition to the heat of condensation of the deposited atoms, the kinetic energies of electrons, sputtered atoms and Argon atoms are additional sources of energy influx to the substrate. The electron density and electron temperatures (kT_e) in the plasma for the conditions used by us are approximately of the order of 10^{10} cm^{-3} and several eV respectively. However these values drop significantly in the region near the substrate, which in our case is located 4 cm away from the target due to which heating from electron is typically not a significant source of energy to promote adatom mobility in the growing thin film. For instance, the electron density has been found to be 5–10% of the concentration in the target region.

The mean free path for a beam of atoms of atomic mass number M_s, passing through a gas of atomic mass number M_g is given by[38]

$$\lambda = \frac{1}{0.25\pi(((d_s+d_g)^2P)/kT)\sqrt{(1+(M_s/M_g))}} \quad (4)$$

where d_s and d_g are the atomic diameters of the sputtered atoms and the sputtering gas, P is the chamber pressure and T is the gas temperature. At chamber pressures of 5 mTorr and higher, the kinetic energies of Argon ions and sputtered atoms (Fig. 3) are greatly reduced due to collisions with the Argon atoms constituting the chamber ambient and the mean free path is reduced. At lower chamber pressures, the kinetic energies of the Ti atoms incident on the film can be significant. In addition, the Ar^+ ions moving at high velocities are reflected toward the film/substrate after neutralization by the cathode. Sputtered atoms undergo more thermalization during the transport process through the plasma to the substrate unlike the neutralized Ar atoms which have longer path lengths (Fig. 3) and retain a significant fraction of their initial energy when they reach the substrate.[39] Due to this, the energies of these reflected neutrals imparted to the film form the most significant contributor to adatom mobility on the surface and atomic peening refers to this phenomenon. The initial energy of the reflected neutral Ar atom is given by the expression.[40]

$$E_i^r = \left[\frac{(M_S - M_g)^2}{(M_S + M_g)^2}\right] V_c \quad (5)$$

where M_S is atomic mass of Ti and M_g is the atomic mass of the gas in the sputtering plasma, which in our case is Ar. V_c stands for the cathode voltage. In this formula, the kinetic energy of reflected neutrals is higher when the atomic mass of the sputtered element is small compared to that of the gas constituting the plasma. In our case, the $M_S - M_g$ difference is *ca.* 7.9. The yield can be estimated from following formula[41]

$$Y_i = 0.42\frac{\alpha^* Q K s_n(\varepsilon)}{U_s[1+0.35U_s s_e(\varepsilon)]}\left[1-\left(\frac{E_{th}}{E}\right)^{1/2}\right]^{2.8} \quad (6)$$

Where 'i' is an index used to denote the particular energetic species (Ti or Ar). U_s is the sublimation energy of titanium. Q and α^* are empirical parameters that are material dependent. E_{th} and E stand for the threshold energy of the process and the reduced energy respectively; $s_e(\varepsilon)$ and $s_n(\varepsilon)$ are Lindhard's inelastic and elastic reduced stopping cross sections.[42] K is a conversion factor that can be calculated from following formula

$$K = 8.478\frac{Z_1 Z_2}{(Z_1^{2/3}+Z_2^{2/3})^{1/2}}\frac{M_1}{M_1+M_2} \quad (7)$$

Here, M_1 and M_2 are mass numbers while Z_1 and Z_2 are the atomic numbers of argon and titanium atoms respectively. The ratio of the energy of the reflected neutral at the deposition substrate (sample) (E_f^r) to its initial energy (E_i^r) is given by[38]

$$\frac{E_f}{E_i} = \exp(-\eta W) \quad (8)$$

where

$$W = 1 - \left\{\frac{(1-M)^2}{2M}\right\}\ln\left\{\frac{(1+M)}{(1-M)}\right\} \quad \text{for} \quad M<1; M=\frac{M_g}{M_s}$$

$$W = 1 - \left\{\frac{(M-1)^2}{2M}\right\}\ln\left\{\frac{(1+M)}{(M-1)}\right\} \quad \text{for} \quad M>1$$

Here, T is the absolute temperature of the gas molecules and k_B is Boltzmann's constant. E_f and E_i are the final initial energy of sputtered atoms, energy when leaving target and energy after collision respectively. If d is the distance between target and sample holder, then η is number of collisions estimated to be d/λ^r. Since it is generally agreed that the major part of the energy imparted to the substrate through atomic peening derives from the reflected neutrals, we used Eqs. (4) through (8), and calculated the relevant parameters for the sputtering process. These parameters are displayed in Table I below.

Films deposited using both DC sputtering and electron beam evaporation at room temperature as well

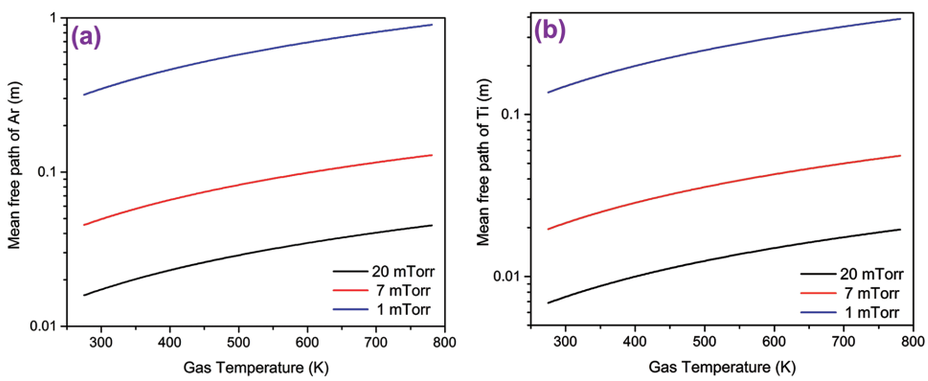

Figure 3. Mean free path of (a) argon atoms and (b) Ti atoms in sputtering system for three different chamber pressures calculated using Eq. (4).

Table I. Calculated yields, mean-free paths and kinetic energies of reflected neutrals.

Chamber pressure (mTorr)	Y_r	$\langle E_i^r \rangle$ (eV)	λ^r (m)	$\langle E_f^r \rangle$ (eV)
1	0.339	3.38	0.343	1.33
7	0.294	2.85	0.053	0.007
20	0.247	2.35	0.025	8.13×10^{-6}

as at 250 °C were found to have good adhesion at 1 mTorr, but not at 20 mTorr. At low pressures the films were so well-adhered that when immersed in an electrolyte they did not delaminate, even at room temperature.

3.3. Effect of Deposition Rate on the Surface Morphology of Ti Films Before Anodization

Equation (9) for the adatom hopping rate (based on the kinetic model) shows a strong relationship between the hopping rate (K_h), the substrate temperature (T_s) and the potential energy barrier to diffusion (E_a)[43]

$$K_h = \nu_{0s} e^{(-E_a/kT_s)} \tag{9}$$

where υ_{0s} is the attempt frequency and k is the Boltzmann constant. From Eq. (9), we see that at high temperatures, adatoms and adparticles species have high mobility. The time required for the growth of one atomic layer is given by[25]

$$\tau_m = \frac{a}{R_{dep}} \tag{10}$$

where a is the average distance between adatoms (approximated by the lattice constant of Ti that is equal to 0.295 nm for a temperature of 25 °C[31]) and R_{dep} is the sputtering rate. When the sputtering rate is 0.23 nm s^{-1} and 0.12 nm s^{-1}, the corresponding growth of one atomic layer requires 1.28 s and 2.46 s respectively. Each adatom needs τ_h seconds to diffuse where τ_h is the inverse of the hopping frequency K_h. Only if τ_h is smaller than τ_m will the adatoms get a chance to diffuse, otherwise they will be buried under the newly arriving adatoms and the probability of diffusion will be decreased.[25]

Ti films sputtered onto silicon at 7 mTorr at 0.23 nm s^{-1} displayed a 3D-hillock, which was absent in the smoother Ti films obtained by sputtering using a lower deposition rate of 0.12 nm s^{-1} (Fig. 4). The cartoons in the foreground of Figures 5(a and b) illustrate how when a high sputtering rate is used, Ti atoms on the surface will be buried under the newly deposited adatoms before they have had a chance to diffuse on the surface thus limiting the hopping rate. This dependence of the film roughness on the deposition rate is captured in Eq. (1) as well, where a higher deposition rate results in a lower surface diffusion length, all other parameters being equal.

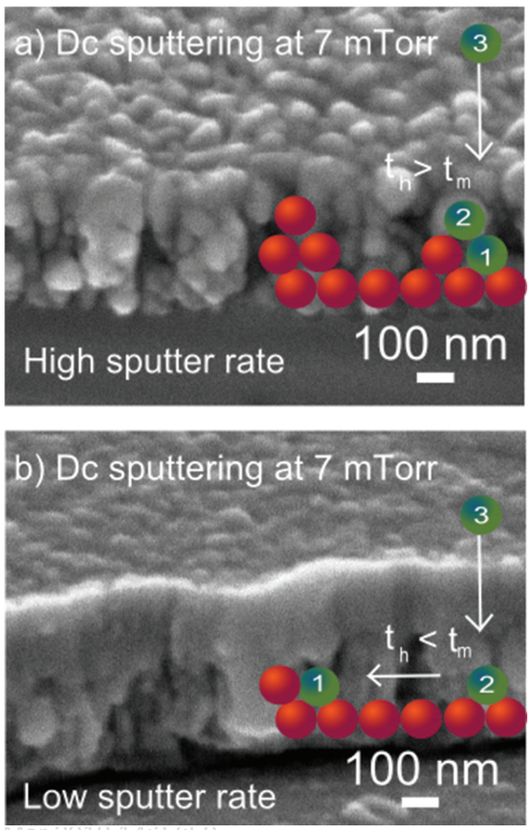

Figure 4. Ti thin films deposited on silicon at a chamber pressure of 7 mTorr using a deposition rate of (a) 0.23 nm s^{-1} and (b) 0.12 nm s^{-1}.

3.4. Morphology of TiO_2 Nanotubes Grown at Elevated Temperature from Non-Atomically Peened Ti Thin Films

As shown previously in Figures 1(c) and 2(c), Ti thin films sputter-deposited at room temperature using chamber pressures of 7 mTorr or higher on substrates such as glass, FTO:glass and quartz, do not benefit from the atomic peening mechanism and are consequently extremely rough with three-dimensional grains of size < 50 nm. When such films are anodized, no discernible ordered nanotube structure is evident; instead a collection of disordered nanopores are seen in both the top-view (Fig. 1(c)) and cross-sectional (Fig. 2(c)) scanning electron micrographs. On the other hand, when Ti is sputter-deposited on to glass substrates heated to temperatures of 150–250 °C while maintaining the chamber pressure at 7 mTorr (Fig. 5(a)), nanotubular structures with a limited amount of order are obtained after electrochemical anodization of the Ti films (Fig. 5(b)). However, when Ti films were deposited on FTO:glass substrates under identical conditions (Fig. 5(c)) and anodized, the resulting structures had poorer order as shown in Figure 5(d). We attribute these variations to differences in surface roughness which in turn influence the tendency to form rough Ti films with three-dimensional protruding grains since microscope slide-type glass substrates used by

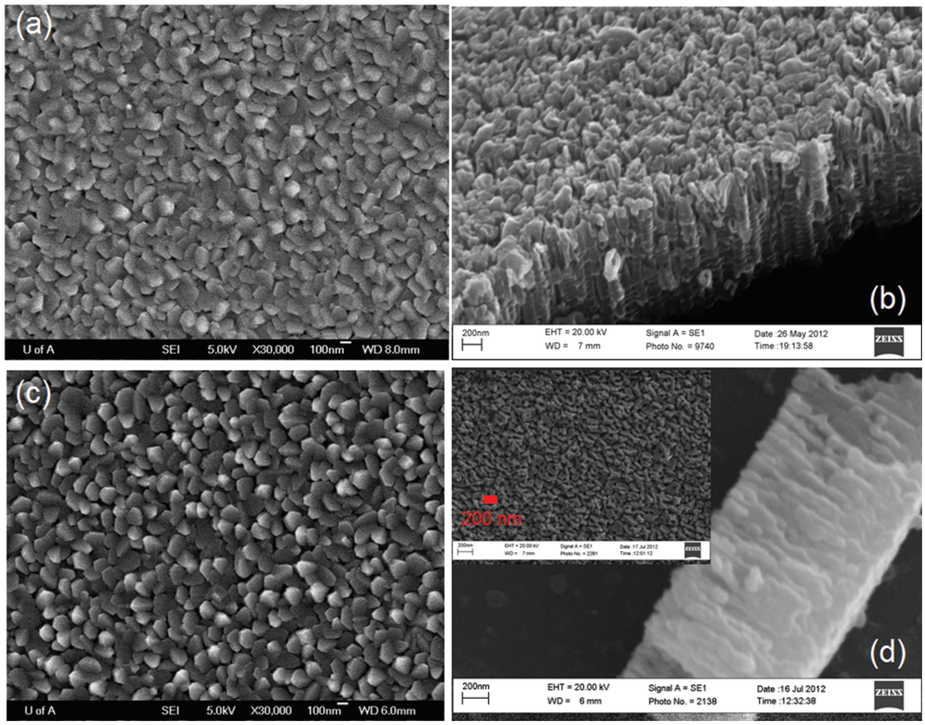

Figure 5. (a, c) FESEM to-view images of 500 nm-thick Ti films sputter-deposited at 7 mTorr at a rate of 0.12 nm s^{-1} on glass and FTO:glass substrates respectively; (b) profile view SEM image of titania nanotubes that resulted from anodization of the Ti film on a glass substrate, shown in part (a); (c) cross-sectional image of the structure resulting from the anodization of the Ti film on FTO:glass shown in part (b) with the inset showing the top-view.

us were smoother with a root mean squared (rms) roughness of 3.4 nm, than FTO:glass substrates (rms roughness of 10.5 nm).

3.5. Morphology of TiO_2 Nanotubes Grown from Atomically Peened Thick Ti Films at Room Temperature

It is easier to obtain TiO_2 nanotubes through the anodization of Ti films of thickness 250–500 nm. As the films get thicker, the surface roughness and overall film non-uniformities increase making it more difficult to obtain an order nanotubular array morphology subsequent to anodization. However, due to the beneficial effect of the atomic peening mechanism, not only are 2 μm-thick Ti films deposited at a chamber pressure of 1 mTorr completely converted into ordered titania nanotube arrays (Fig. 6), but the entire deposition process can be performed at room temperature without any recourse to substrate heating or additional ion bombardment.

3.6. How Important is Crystallographic Orientation?

Crawford and Chawla,[44] and Leonardi et al.[45] used EBSD studies to elegantly demonstrate the importance of the crystallographic orientation of individual grains in determining the growth of TiO_2 nanotubes. Specifically, it was shown that the formation of titania nanotubes by anodization was retarded on the basal (001) planes in comparison to (010), (110) and (111) planes.[44,45] However, to provide some context, the aforementioned studies used Ti foils with large, flat grains of size 10 μm–100 μm and exclusively employed aqueous electrolytes for anodization. Whether or not crystallographic orientation plays a similarly outsized role in the anodization of vacuum deposited Ti thin films where the grain sizes are in the range 50 nm–300 nm (such as those studied in this report), remains an open question. We have observed a much stronger effect of the Ti film roughness on the morphology of the resulting TiO_2 nanotubes, which may be reconciled with the crystallographic dependence of nanotube formation as follows: when the grains are not flat but are instead three-dimensional and protrude out of the substrate, such as in Figure 1(a), different crystal planes are simultaneously accessible to the ions responsible for field-assisted oxidation, field-assisted etching and chemical dissolution, and hence a single crystal plane cannot inhibit pore formation. Thus in Figure 7, we see that the dominant crystallographic orientation in Ti thin films deposited on glass and Si substrates are different (glass being less optimal due to basal plane texture), and yet nanotubes are formed upon anodization in both cases.[23] We showed in this report that ordered nanotube formation is determined more by the chamber pressure during sputtering (i.e., the presence or absence of

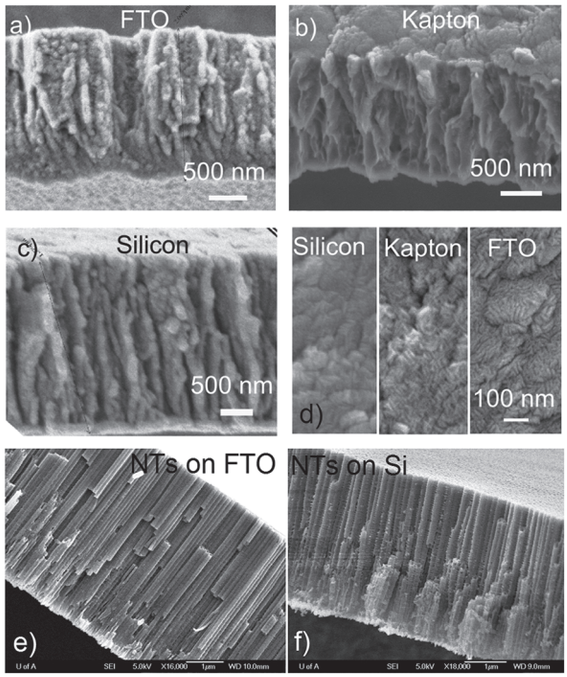

Figure 6. (a–c) Cross-sectional FESEM images of 2 μm-thick Ti films deposited on to FTO; glass, Kapton$^{(R)}$ (polyimide) and Si wafer substrates respectively at a deposition rate of 0.12 nm s^{-1}; (d) magnified top-views of the 2 μm-thick Ti films deposited on Si, Kapton$^{(R)}$ (polyimide) and FTO:glass substrates respectively; (e, f) ordered TiO_2 nanotube arrays on FTO:glass and Si wafer respectively resulting from anodization of the films shown in parts (a), (c) and (d).

the atomic peening mechanism) with the substrate being a secondary factor. Furthermore, Ti thin films were anodized by us in EG-based organic electrolytes, which unlike aqueous electrolytes, typically result in nanotubes arranged in honeycomb-like triangular lattices. It is therefore unclear at the present moment whether the significant retardation of nanotube growth observed on basal planes on large-grained Ti foils in aqueous anodization electrolytes extends to small-grained vacuum deposited Ti thin films anodized in organic electrolytes.

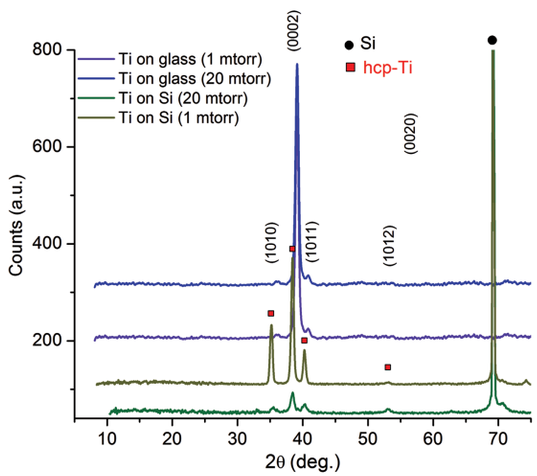

Figure 7. Effect of substrate on the crystallographic texture of sputtered Ti films under identical conditions. Powder mode X-ray diffractograms of Ti thin films deposited on to glass and silicon substrates using DC magnetron sputtering at two different chamber pressures (1 mTorr and 20 mTorr). Reprinted with permission from [23], S. Farsinezhad, et al., *Phys. Status Solidi A* 211, 113 (**2014**). © 2014, John Wiley & Sons.

4. CONCLUSION

The anodic growth dynamics of TiO_2 nanotubes on native and non-native substrates are fundamentally different in terms of one measure, namely the grain size of the precursor Ti substrate used for electrochemical anodization. Hot rolled Ti foils have large flat grains 10–100 μm in size while vacuum deposited Ti thin films have grain sizes that are orders of magnitude smaller and multiple orientations, some of which are not orthogonal to the substrate. We showed that even when quartz substrates are maintained at a temperature of 700 °C during the sputter deposition of Ti, the grain size is merely a few hundred nanometers, pointing both to the relative inefficiency in using substrate heating in increasing the grain size and the fundamental difference between anodization of Ti foils and of vacuum deposited Ti films. Ti thin films sputter-deposited at room temperature at chamber pressures of 7 mTorr or higher resulted in disordered and irregular nanoporous structures instead of nanotube arrays when anodized in fluoride-containing ethylene glycol-based organic electrolytes. Atomic peening enabled large-grained Ti films with low surface roughness to be obtained even for film thickness as high as 2 μm when sputtering was performed at lower chamber pressures (~1 mTorr) at room temperature, and resulted in highly ordered nanotube arrays with smooth sidewalls when anodized. Evaporated Ti films formed nanotube arrays with rough, highly ridged, sidewalls. By varying the conditions of thin film growth over a large range of parameters, and correlating the structure and morphology of the thin films obtained to the nanostructures that resulted upon anodization, we obtain the insight that the formation of ordered nanotube arrays as opposed to disordered and irregular nanoporous structures, depends critically on the pore nucleation processes, which in turn depend on the surface roughness and grain structure of the precursor Ti films.

Acknowledgments: All authors thank NSERC, NRC-NINT and CMC Microsystems for direct and indirect financial support. We acknowledge the staff of the UofA Nanofab for technical assistance. We thank Professor David Mitlin and Dr. Eric Luber for depositing Ti films at 700 °C on quartz substrates and also acknowledge the collection of some FESEM images by Dr. Xiaojiang (Albert) Zhang.

References and Notes

1. J. Wang and Z. Q. Lin, *Chem. Mater.* 20, 1257 (**2008**).
2. J. Wang and Z. Q. Lin, *J. Phys. Chem. C* 113, 4026 (**2009**).

3. O. K. Varghese, G. K. Mor, C. A. Grimes, M. Paulose, and N. Mukherjee, *J. Nanosci. Nanotechnol.* 4, 733 (**2004**).
4. O. K. Varghese, M. Paulose, K. Shankar, G. K. Mor, and C. A. Grimes, *J. Nanosci. Nanotechnol.* 5, 1158 (**2005**).
5. T. Maiyalagan, B. Viswanathan, and U. V. Varadaraju, *J. Nanosci. Nanotechnol.* 6, 2067 (**2006**).
6. Q. Wang, Z. H. Wen, and J. H. Li, *J. Nanosci. Nanotechnol.* 7, 3328 (**2007**).
7. A. Ghicov and P. Schmuki, *Chem. Commun. (Cambridge, U. K.)* 20, 2791 (**2009**).
8. D. S. Guan, C. A. Cai, and Y. Wang, *J. Nanosci. Nanotechnol.* 11, 3641 (**2011**).
9. P. Roy, S. Berger, and P. Schmuki, *Angew. Chem.-Int. Edit.* 50, 2904 (**2011**).
10. P. Kar, A. Pandey, J. J. Greer, and K. Shankar, *Lab Chip* 12, 821 (**2012**).
11. G. K. Mor, O. K. Varghese, M. Paulose, K. Shankar, and C. A. Grimes, *Sol. Energy Mater. Sol. Cells* 90, 2011 (**2006**).
12. K. Shankar, J. I. Basham, N. K. Allam, O. K. Varghese, G. K. Mor, X. J. Feng, M. Paulose, J. A. Seabold, K. S. Choi, and C. A. Grimes, *J. Phys. Chem. C* 113, 6327 (**2009**).
13. K. Shankar, TiO_2 Nanotube Arrays: Growth and Application, Encyclopedia of Nanotechnology, edited by B. Bhushan, Springer Netherlands (**2012**), p. 2742
14. K. Shankar, Templating and Pattern Transfer Using Anodized Nanoporous Alumina/Titania, Nanofabrication, edited by M. Stepanova and S. Dew, Springer, Vienna (**2012**), p. 321
15. J. Bandara, K. Shankar, J. Basham, H. Wietasch, M. Paulose, O. K. Varghese, C. A. Grimes, and M. Thelakkat, *Eur. Phys. J.-Appl. Phys.* 53, 20601 (**2011**).
16. O. K. Varghese, M. Paulose, and C. A. Grimes, *Nat. Nanotechnol.* 4, 592 (**2009**).
17. G. K. Mor, O. K. Varghese, M. Paulose, and C. A. Grimes, *Adv. Funct. Mater.* 15, 1291 (**2005**).
18. S. Berger, A. Ghicov, Y. C. Nah, and P. Schmuki, *Langmuir* 25, 4841 (**2009**).
19. C. K. Xu, P. H. Shin, L. L. Cao, J. M. Wu, and D. Gao, *Chem. Mater.* 22, 143 (**2010**).
20. V. Galstyan, A. Vomiero, E. Comini, G. Faglia, and G. Sberveglieri, *RSC Adv.* 1, 1038 (**2011**).
21. V. Galstyan, A. Vomiero, I. Concina, A. Braga, M. Brisotto, E. Bontempi, G. Faglia, and G. Sberveglieri, *Small* 7, 2437 (**2011**).
22. A. Vomiero, V. Galstyan, A. Braga, I. Concina, M. Brisotto, E. Bontempi, and G. Sberveglieri, *Energ. Environ. Sci.* 4, 3408 (**2011**).
23. S. Farsinezhad, A. N. Dalrymple, and K. Shankar, *Phys. Status Solidi A* 211, 1113 (**2014**).
24. S. L. Marasso, G. Canavese, and M. Cocuzza, *Microelectron. Eng.* 88, 2322 (**2011**).
25. L. Abelmann and C. Lodder, *Thin Solid Films* 305, 1 (**1997**).
26. S. Farsinezhad, A. Mohammadpour, A. N. Dalrymple, J. Geisinger, P. Kar, M. J. Brett, and K. Shankar, *J. Nanosci. Nanotechnol.* 13, 2885 (**2013**).
27. E. G. Wang, B. G. Liu, J. Wu, M. Z. Li, J. X. Zhong, J. Wendelken, Q. Niu, and Z. Zhang, *Comp. Mater. Sci.* 23, 197 (**2002**).
28. H. D. Zheng, A. Z. Sadek, M. Breedon, D. Yao, K. Latham, J. du Plessis, and K. Kalantar-Zadeh, *Electrochem. Commun.* 11, 1308 (**2009**).
29. M. Paulose, K. Shankar, S. Yoriya, H. E. Prakasam, O. K. Varghese, G. K. Mor, T. A. Latempa, A. Fitzgerald, and C. A. Grimes, *J. Phys. Chem. B* 110, 16179 (**2006**).
30. D. L. Smith, Thin-Film Deposition: Principles and Practice, McGraw-Hill, New York etc (**1995**), Vol. 108.
31. R. M. Wood, *P. Phys. Soc.* 80, 783 (**1962**).
32. D. Vick, L. J. Friedrich, S. K. Dew, M. J. Brett, K. Robbie, M. Seto, and T. Smy, *Thin Solid Films* 339, 88 (**1999**).
33. Z. Szczudło, A. Ciszewski, and Y. B. Losovyj, *Appl. Surf. Sci.* 174, 138 (**2001**).
34. T. Biernat and A. Dąbrowski, *Vacuum* 63, 113 (**2001**).
35. T. Hammerschmidt, A. Kersch, and P. Vogl, *Phys. Rev. B* 71, 205409 (**2005**).
36. K. N. Chappanda, Y. R. Smith, L. W. Rieth, P. Tathireddy, M. Misra, and S. K. Mohanty, *IEEE T. Nanotechnol.* 14, 18 (**2015**).
37. H. Kersten, G. M. W. Kroesen, and R. Hippler, *Thin Solid Films* 332, 282 (**1998**).
38. B. Window and K. H. Müller, *Thin Solid Films* 171, 183 (**1989**).
39. J. C. Moreno-Marín, I. Abril, A. Gras-Marti, V. Konoplev, J. J. Jiménez-Rodriguez, and A. M. C. Pérez-Martin, *Vacuum* 45, 1135 (**1994**).
40. J. Musil, J. Sicha, D. Herman, and R. Cerstvy, *Journal of Vacuum Science and Technology A* 25, 666 (**2007**).
41. I. Kolev and A. Bogaerts, *Journal of Vacuum Science and Technology A* 27, 20 (**2009**).
42. P. Sigmund, *Physical Review* 184, 383 (**1969**).
43. E. Rabani, J. D. Gezelter, and B. J. Berne, *J. Chem. Phys.* 107, 6867 (**1997**).
44. G. A. Crawford and N. Chawla, *Scr. Mater.* 60, 874 (**2009**).
45. S. Leonardi, A. Li Bassi, V. Russo, F. Di Fonzo, O. Paschos, T. M. Murray, H. Efstathiadis, and J. Kunze, *The Journal of Physical Chemistry C* 116, 384 (**2011**).

Received: 24 May 2016. Accepted: 16 June 2016.